Mini-CHT powered Formation Flying Mission for Magnetic Reconnection Research in Space

IEPC-2019-377

Presented at the 36th International Electric Propulsion Conference
University of Vienna • Vienna, Austria
September 15-20, 2019

Jacob Simmonds[1]
Princeton University, Princeton, NJ 08544, USA

Masaaki Yamada[2] and Yevgeny Raitses[3]
Princeton Plasma Physics Laboratory, Princeton, NJ 08544, USA

Abstract: It has long been suggested that formations of small satellites can achieve the same capability as a large satellite for a fraction of the cost. One such mission has been proposed by PPPL[1] to take time and spatial measurements of plasma properties during magnetic reconnection in the magnetosphere using a fleet of 100 CubeSats and a single command satellite. For a preliminary test of this concept, a fleet of 8 6U CubeSats is studied. The basic cost analysis priced this mission at $42 million, in contrast to the similar MMS mission which was $1.1 billion[2]. While the capabilities of these missions differ, this presents a much cheaper alternative to traditional NASA missions and is possible due to the low power electric propulsion that will maintain the formation. A mission analysis was conducted using numerical simulation techniques for the low-thrust transfers[3,4] and analytic orbital element models for formation-keeping. A detailed explanation of how the thruster parameters were selected is described by consolidating several works on low-thrust maneuvers and orbital perturbations.

Nomenclature

PPPL	=	Princeton Plasma Physics Laboratory
a	=	semimajor axis of orbit
e	=	eccentricity of orbit
i	=	inclination of orbit
ω	=	argument of perigee of orbit
Ω	=	right ascension of the ascending node
r_p	=	perigee of the orbit
r_a	=	apogee of the orbit
θ	=	true anomaly of the orbit
M	=	mean anomaly of the orbit
U	=	gravitational potential
J_2	=	oblateness constant of the Earth
R_E	=	radius of the Earth
n	=	rate of orbit
I_{sp}	=	specific Impulse
η	=	thruster efficiency

[1] PhD Candidate, Mechanical and Aerospace Engineering, jacobbs@princeton.edu
[2] Principal Research Physicist, Plasma Science and Technology, myamada@pppl.gov
[3] Principal Research Physicist, Plasma Science and Technology, yraitses@pppl.gov

I.Introduction

Miniaturized satellite technology has created new interest in formations of small satellites due to the decreased cost associated with mass savings. These formations require some form of propulsion to not only maintain the formation but transfer the orbit over the mission. While this presents an opportunity for those who work in the field of plasma propulsion, it is not always so clear how to extract the necessary thruster parameters (thrust, Isp, power) from the proposed mission. Similarly, once a mission has been envisioned it can be unclear what type of thruster will allow the mission to be viable.

A comprehensive analysis of a low-thrust electric propulsion mission requires significant analysis of the optimal trajectory of the satellite to maximize fuel use, minimize time in radiation belts, and ensure the solar panels obtain sufficient power generation. While such analyses must eventually happen, an initial pen-to-paper viability check is helpful to determine the approximate satellite size and thruster parameters a mission would need. Such pen-to-paper design is again difficult for low-thrust propulsion as it lacks the simplicity of the analytic expressions found in high-impulse maneuvers, however it is possible to obtain semi-analytic expressions of many forms of orbital maneuvers, which have been compiled here and used to calculate the delta V and specific impulse required for each satellite thruster in the formation.

An attempt to illustrate a thruster-selection process is demonstrated in the context of a multi-satellite formation mission currently being discussed in the Princeton Plasma Physics Laboratory (PPPL).[1] The mission revolves around measuring the phenomenon of magnetic reconnection, which occurs when magnetic field lines splice together in a plasma, resulting in a transformation of magnetic energy to thermal and kinetic energy of ions and electrons. While this has been studied in an experimental setting, such as the "Magnetic Reconnection Experiment" and "FLARE" in PPPL, there is a need to match the theory with reconnection that occurs naturally, notably in the magnetopause between the Earth and Sun. This presents a great challenge, as the magnetopause occurs at an altitude of 63,000 km above the Earth. A previous mission to measure this region by NASA – the Magnetospheric Multiscale Mission (MMS) – was composed of 4 satellites and had a budget of $1.1 billion. While the data collected made great strides in the theory of reconnection, to fully capture the physics of magnetic reconnection would require a much larger formation for spatial measurements of the plasma properties. This presents an opportunity for small satellites such as CubeSats to lower the cost of a mission sufficiently that a very large formation (up to 100 satellites) may be attempted for an order of magnitude lower cost than MMS.

This work is split into three parts. The first outlines the basic orbital elements required to create the desired formation at the target orbit, the second considers the orbital perturbations the formation will experience and the corrections to the initial orbital elements to minimize the thrust required as well as the thrust and Delta V needed to maintain the formation. Finally, the third outlines a method to determine the time, Delta V, and the basic cost analysis to use onboard thrusters to transfer from an initial orbit, such as an ISS orbit in LEO, to the target final orbit. This analysis is intended to be a first-stage mission analysis as there is no attempt to optimize any of these parts.

II.Orbital Elements for a Formation

The commonly used system to express position and velocity coordinates of satellites is the Keplerian orbital elements, pictured in Fig. 1. These represent a convenient way to determine the osculating (unchanging without perturbations) orbit of any satellite, where the only changing parameter is the angle about the orbit – the true anomaly (θ). An expression to derive the orbital elements of any satellite as well as any other satellite of known position in the Clohessy Wiltshire frame of reference (Figure 2) is derived in Eq. 1.

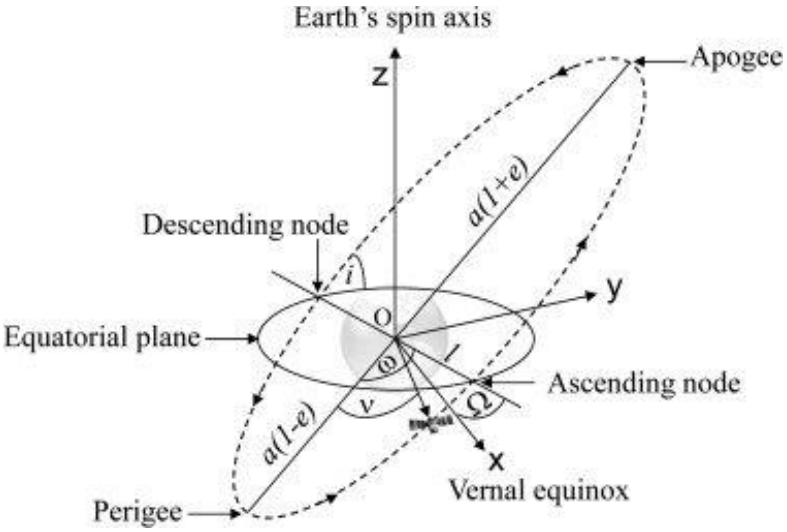

Figure 1. Keplerian Orbital Elements (CC BY-NC-ND 3.0

The Supercluster mission being considered by PPPL calls for, at minimum, a cube of 8 satellites each at least 100km apart (and ideally a 3d-grid of >100 satellites) to measure the plasma properties at the magnetopause with a formation that needs to maintain for 3 years. The magnetopause exists 70,000 km from Earth (11 Earth Radii), which presents problems for communication from small, low power satellites. Lowering the perigee of the orbit to roughly 400km altitude then allows standard CubeSat communication equipment to be utilized. The desired orbit will then have a high eccentricity of 0.8238 (Fig. 2).

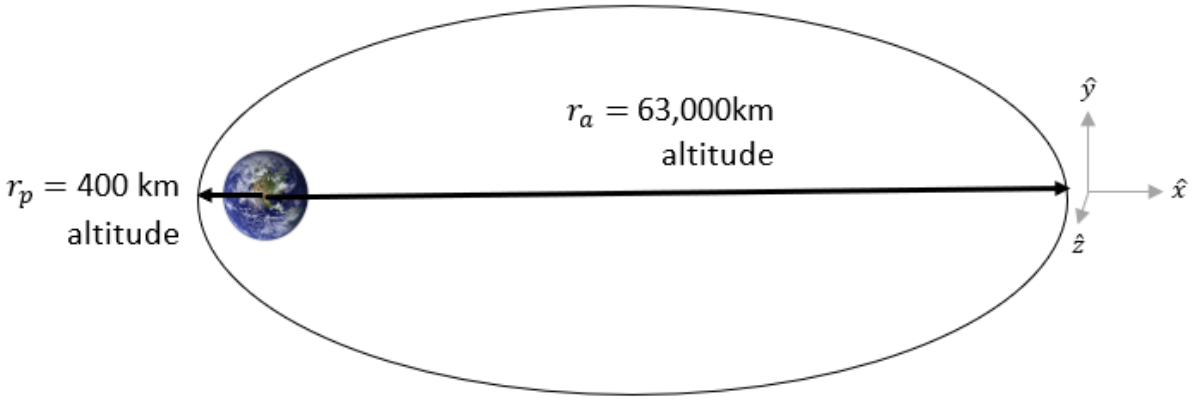

Figure 2. Orbit of the supercluster mission with Clohessy-Wiltshire reference frame

Fortunately the formation needs to only exist at apogee – the satellites can drift relative to each other as long as they return to the intended position when measurements need to be taken. As such, by ensuring the orbital period of each satellite is the same, the formation should return to its initial shape. Note there will be some relative shift of orbital elements due to perturbations, but this will be handled in section 2. As a first pass, to keep the same orbital period we only need to ensure the semimajor axis is the same. Thus, if we consider the center satellite as our master satellite, we can use the Clohessy-Wiltshire reference frame (Figure 2) to define the relative (x, y, z) position of our satellites from our master and determine the new orbital elements. This is a relatively simple problem for a 2d formation (x, y), however including a z term makes things somewhat more complicated. An analytical solution is possible, however, and is presented below, as well as a simpler small-angle solution.

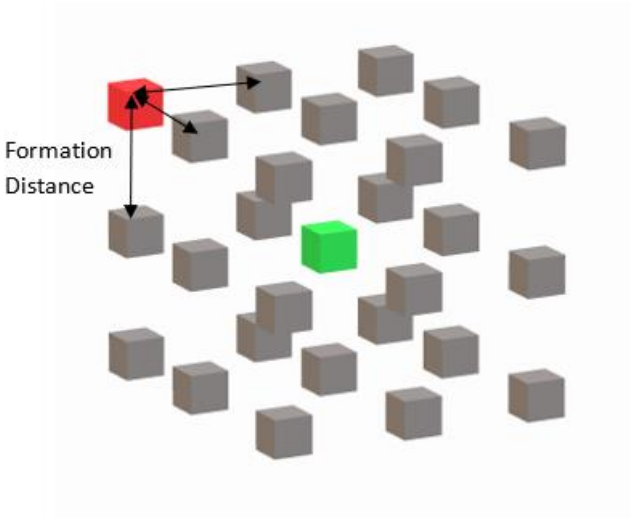

Figure 3. 27 satellite formation at apogee with center (green) and corner (red) satellites highlighted. Not to scale.

The following is solved for the formation existing at apogee, but the same equations can be used by replacing the ra0 term with the radius at the desired true anomaly $r = \frac{a(1-e^2)}{a+e\cos\theta}$. In either case, we determine the change in argument of perigee, ω1, in an intermediate orbit if z=0. We then define a new angle α which is the shift from the intermediate orbit to achieve the desired z position. Figure X shows the geometry of the problem.

For the intermediate orbit, or for a formation where z=0, it is relatively simple to determine the orbital elements. If a satellite is further along or behind in the orbit, but with the same mean anomaly (orbiting in sync), then it must have a different argument of perigee (ω). Similarly, if a satellite is further or closer out, but the semimajor axis cannot change, then this change needs to occur from the eccentricity.

With a shift in z it becomes much more complicated. As the orbital elements are rotations from the cartesian Earth-fixed frame to the perifocal, our local rotation angle needs to be converted. To do this we can utilize the usual $R_z(\Omega_0)$, $R_z(i_0)$, $R_z(\omega_1)$ rotation matrices to transform from the Earth Fixed frame to the Perifocal frame, but with an additional Ry(α) to achieve our new orbital elements. We can then set this matrix equal to a typical $R_z(\Omega_2)$, $R_z(i_2)$, $R_z(\omega_2)$ transformation to determine the relation between the orbital elements and the master satellite with a shift in position. As we are rotating α relative to our intermediate orbit, we must use ω_1 in this expression.

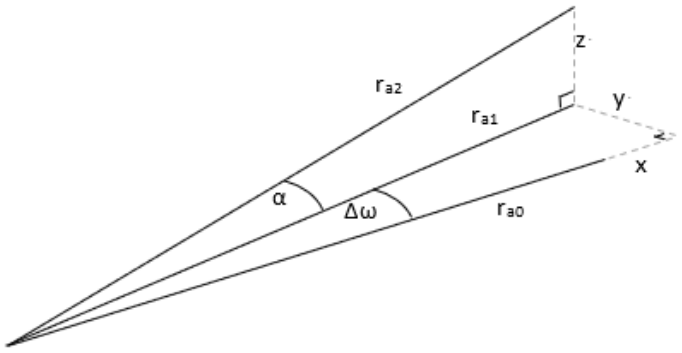

Figure 4. Geometry of the satellite relative positions

General Form:

$$a_1 = a_0 = a \tag{1}$$

$$r_{a0} = a_0(1 + e_0) \tag{2}$$

$$e_2 = \frac{\sqrt{(x+r_{a0})^2+y^2+z^2}}{a_2} - 1 \tag{3}$$

$$\alpha = \tan^{-1}\left(\frac{z}{\sqrt{(r_{a0}+x)^2+y^2}}\right) \tag{4}$$

$$\omega_1 = \omega_0 + \tan\left(\frac{y}{r_{a0}+x}\right) \tag{5}$$

$$i_2 = \arccos(cos(i_1)\,cos(\alpha) + sin(i_1)\,sin(\alpha)\,sin(\omega_1)) \tag{6}$$

$$\omega_2 = \arctan\big(\cos(\alpha)\,\tan(\omega_1) - \sin(\alpha)\,\cot(i_1)\,\sec(\omega_1)\big) \tag{7}$$

$$\Omega_2 = \arctan\left(tan(\Omega_1) - \frac{\sec^2\Omega_1}{cos(i_1)\,tan(\omega_1)+tan(\Omega_1)-cot(\alpha)\,sec(\omega_1)\,sin(i_1)}\right) \tag{8}$$

Assuming small angle form ($z, x, y \ll r_{a0}$) and $\omega_1, i_1 \neq 0$), one can use a Taylor series expansion on the inverse trigonometric functions (Eq. 4,6,7,8) and eliminate the higher order terms to obtain:

$$\alpha = \frac{z}{r_{a0}} \tag{9}$$

$$e_2 = \frac{x+r_{a0}}{a_2} - \tag{10}$$

$$\omega_1 = \omega_0 + \frac{y}{r_{a0}} \tag{11}$$

$$i_2 = i_1 - \frac{z\,sin(\omega_1)}{r_{a0}\,sin(i_1)} \tag{12}$$

$$\omega_2 = \omega_1 - \frac{z\,\cos\omega_1}{r_{a0}\tan i_1} \tag{13}$$

$$\Omega_2 = \Omega_1 + \frac{z\cos(\omega_1)}{r_{a0}\,sin(i_1)} \tag{14}$$

For our supercluster mission, the orbital elements for the highlighted satellites in the center and corner from Fig. 3 is shown in Table 1. The relevant orbital elements for a satellite in the center and a corner satellite are shown in Table 1. Elements are found both using the general expression and the small angle approximation to 5 decimal places to show the expected differences for such an orbit.

Table 1. Orbital Elements for a central and corner satellite with formation distance of 50 km

Orbital Element	Center Satellite	Corner Satellite (General)	Corner Satellite (Small Angle Approximation)
a	38,247 km	38,247 km	38,247 km
e	0.82380	0.82511	0.82511
i	51.6º	51.60000º	51.60000º
ω	0º	0.00854º	0.00852º
Ω	20º	20.05237º	20.05240º

III.Orbital Perturbations

A. J2 and third body effects

A satellite in orbit experiences a large variety of forces unaccounted for in a simple Keplerian orbit. These forces can range from the Sun and Moon's gravity, solar radiation pressure, the unevenness of the Earth's gravitational field,

and atmospheric drag. To account for these forces one can continue using the osculating orbital elements ascribed from a Keplerian orbit, but with a slight time dependence due to these orbital perturbations. By adding a perturbing force when solving for the orbital elements one can derive these time dependencies. However, the form of the perturbation becomes important – if the perturbing force is derivable from a potential, the approach taken to achieve Lagrange's Planetary Equations is applicable. If it is not, then Gauss's Variational Equations can be used. For the case of gravitational perturbations such as the Earth's uneven gravitational field, the moon's gravity, and the Sun's gravity, Lagrange's Planetary Equations hold. The latter case will be analyzed next.

$$\dot{a} = \frac{2}{na}\frac{2}{na}\frac{\partial U_1}{\partial M} \tag{15}$$

$$\dot{e} = \frac{1-e^2}{na^2 e}\left(\frac{\partial U_1}{\partial M} - (1-e^2)^{-\frac{1}{2}}\frac{\partial U_1}{\partial \omega}\right) \tag{16}$$

$$\dot{I} = \frac{1}{na^2\sqrt{1-e^2}}\left(\cot I \frac{\partial U_1}{\partial \omega} - \csc I \frac{\partial U_1}{\partial \Omega}\right) \tag{17}$$

$$\dot{\omega} = \frac{(1-e^2)^{\frac{1}{2}}}{na^2 e}\frac{\partial U_1}{\partial e} - \frac{\cot I}{na^2(1-e^2)^{\frac{1}{2}}}\frac{\partial U_1}{\partial M} \tag{18}$$

$$\dot{\Omega} = \frac{\csc I}{na^2(1-e^2)^{\frac{1}{2}}}\frac{\partial U_1}{\partial M} \tag{19}$$

$$\dot{M} = n - \frac{2}{na}\frac{\partial U_1}{\partial a} - \frac{1-e^2}{na^2 e}\frac{\partial U_1}{\partial e} \tag{20}$$

Where a is the semimajor axis, n is the mean angular motion of the satellite, U_1 is the perturbing potential, M is the mean anomaly, e is the eccentricity, ω is the argument of perigee, I is the inclination, and Ω is the right ascension of the ascending node.

These expressions contain the partial derivative of the disturbing potential relative to the orbital elements, and so some work needs to be done to derive the orbital element drift for each case (Earth, moon, Sun). While the latter two are just dependent on geometry, solving for the Earth's uneven field perturbation involves breaking down the shape of the Earth into spherical harmonics using the orbital element coordinate system and then solving for the magnitude of each harmonic. It turns out that for Earth, the J2 perturbation – which is a measure of how oblate the Earth is – has the largest magnitude by several orders, and so we will only consider it here. Considering just Earth's oblateness, the new gravitational potential is:

$$U(r,\phi) = \frac{\mu}{r}\left(1 - J_2\left(\frac{R_E}{r}\right)^2\left(\frac{3}{2}\cos^2\phi - \frac{1}{2}\right)\right) \tag{21}$$

Where ϕ is the co-latitude ($\phi = 90 - latitude$). The common literature value for J2 is 0.001082628. Solving for the perturbing potential in orbital elements:

$$U_1 = -\frac{\mu J_2 R_E^2}{a^3(1-e^2)^{\frac{3}{2}}}\left(\frac{3}{4}\sin^2 I - \frac{1}{2}\right) \tag{22}$$

The partial derivatives of this can then be inserted into Lagrange's Planetary Equations to provide the following expressions. Note that these expressions are time averaged over the orbit.

Table 2. Orbital Element Variations from J2 Perturbation

Element	J2 Perturbation
$\dot{a}$	0
$\dot{e}$	0
$\dot{I}$	0
$\dot{\omega}$	$\frac{3}{2}J_2 n\left(\frac{R_E}{a(1-e^2)}\right)^2\left(2-\frac{5}{2}\sin^2 I\right)$
$\dot{\Omega}$	$-\frac{3}{2}J_2 n\left(\frac{R_E}{a(1-e^2)}\right)^2\cos I$
$\dot{M}$	$n\left(1+\frac{3}{4}J_2\left(\frac{R_E}{a(1-e^2)}\right)^2\sqrt{1-e^2}(3\cos^2 I-1)\right)$

Also included are the Moon and Sun's orbital element perturbations. These expressions were obtained from the work of Ref. 5, which derived the semi-analytic osculating orbital elements from a third gravitational body. The approximations involved assuming the third body's orbital radius is much larger than the satellite's orbital radius. The expressions are slightly altered to fit the other expressions in this work.

Table 3. Orbital Element Variations from Third Body Perturbation

Element	Sun/Moon Perturbation
$\dot{a}$	0
$\dot{e}$	$\frac{15\mu' n'^2 e\sqrt{1-e^2}}{8n}\left(1+\frac{3}{2}e'^2+\frac{15}{8}e'^4\right)\sin^2 I\sin(2\omega)$
$\dot{I}$	$\frac{-15\mu' n'^2 e^2}{16n\sqrt{1-e^2}}\left(1+\frac{3}{2}e'^2+\frac{15}{8}e'^4\right)\sin(2I)\sin(\omega)$
$\dot{\omega}$	$\frac{3\mu' n'^2}{8n\sqrt{1-e^2}}\left(1+\frac{3}{2}e'^2+\frac{15}{8}e'^4\right)\left((5\cos^2 I-1+e^2)+5\cos(2\omega)\,(1-e^2-\cos^2 I)\right)$
$\dot{\Omega}$	$\frac{3\mu' n'^2\cos i}{8n\sqrt{1-e^2}}\left(1+\frac{3}{2}e'^2+\frac{15}{8}e'^4\right)(5e^2\cos(2\omega)-3e^2-2)$
$\dot{M}$	$n\left(1+\frac{\mu' n'^2}{8n}\left(1+\frac{3}{2}e'^2+\frac{15}{8}e'^4\right)\left((3e^2+7)(3\cos^2 I-1)+15(1+e^2)\sin^2 I\cos^2\omega\right)\right)$

Note: Terms with ' are those of the third body: e.g. e' is eccentricity of the third body. By inserting the orbital elements in the desired orbit, the magnitude of the changes in orbital elements can be found for the formation (Table 4).

Table 4. Magnitude of Orbital Element Perturbations from J2, Moon, and Sun Influence on formation in Target Orbit

Element	J2 Perturbation		Moon Perturbation		Sun Perturbation	
	Center Satellite	Corner-Center	Center Satellite	Corner-Center	Center Satellite	Corner-Center
$\dot{a}$ (year^{-1})	0	0	0	0	0	0
$\dot{e}$ (year^{-1})	0	0	$2.4894*10^{-5}$	$-1.973*10^{-5}$	$5.810*10^{-6}$	$-4.604*10^{-9}$
$\dot{I}$ (rad/year)	0	0	$-5.058*10^{-5}$	$3.999*10^{-5}$	$-1.180*10^{-8}$	$9.333*10^{-9}$
$\dot{\omega}$ (rad/year)	-0.539939	$-7.323*10^{-3}$	0.02745	$-9.231*10^{-5}$	$6.41*10^{-6}$	$-2.154*10^{-9}$
$\dot{\Omega}$ (rad/year)	-0.721932	$9.791*10^{-3}$	-0.00853	$-1.149*10^{-4}$	$-1.990*10^{-6}$	$6.700*10^{-9}$
$\dot{M}$ (rad/year)	0.2844	$2.889*10^{-3}$	0.06816	$8.436*10^{-5}$	$1.591*10^{-5}$	$1.969*10^{-8}$

Table 4 reveals the largest influence on the orbit is due to the J2 perturbation, both by the bulk movement of the entire formation and the drift between the satellites within. This is followed by the effect of the Moon, while the sun has negligible effect. The drift between satellites of mean anomaly is problematic as this represents satellites moving faster about the orbit, vastly changing the formation distance and shape. However by altering the orbital rate of these drifting satellites by changing the semimajor axis, it may be possible to eliminate this drift. A short analysis of $\dot{M}$ matching is presented later in this paper once the $\dot{M}$ from air drag is determined. Thruster Delta V's required to counteract the relative drift of the other orbital elements are also calculated.

B. Air Drag

To determine the effect of air drag one must take a different approach to determine the osculating orbital elements. As the force is not derivable from a potential, we shall use Gaussian perturbation equations, which allow a form of the changing orbital elements to be found based on known force vectors. The difficulty in determining the solution in this case comes from the form of the drag force – as it is dependent on the orbital radius and speed of the spacecraft the typical approach of assuming a small eccentricity does not hold. As we must integrate over the orbital period to find the average change in orbital elements this can present a challenge. Gauss's variational equations follow, with the force vector defined as (F_r, F_θ, F_z) corresponding to the radial component, the azimuthal which in this case is the in-plane component perpendicular to the radius, and the component normal to the orbital plane.

$$\dot{a} = \frac{2}{n\sqrt{1-e^2}}\left(e \sin\theta\, F_r + \frac{a(1-e^2)}{r} F_\theta\right) \tag{23}$$

$$\dot{e} = \frac{\sqrt{1-e^2}}{na}\left(\sin\theta\, F_r + \left(\cos\theta + \frac{e+\cos\theta}{1+e\cos\theta}\right) F_\theta\right) \tag{24}$$

$$\dot{I} = \frac{r\cos(\omega+\theta)}{na^2\sqrt{1-e^2}} F_z \tag{25}$$

$$\dot{\omega} = \frac{\sqrt{1-e^2}}{nae}\left(-\cos\theta\, F_r + \sin\theta\left(1 + \frac{r}{a(1-e^2)}\right) F_\theta\right) - \frac{r\cot i \cot(\omega+\theta)}{\sqrt{(a(1-e^2)\mu}} F_z \tag{26}$$

$$\dot{\Omega} = \frac{r\sin(\omega+\theta)}{na^2\sqrt{1-e^2}\sin I} F_z \tag{27}$$

$$\dot{M} = \frac{1}{na^2 e}\left((a(1-e^2)\cos\theta - 2er)F_r - (a(1-e^2)+r)\sin\theta\, F_\theta\right) \tag{28}$$

We assume the air drag force has the standard drag equation form, where the density profile follows an isothermal atmospheric density model with variable solar EUV flux and geomagnetic activity.[6]

$$\vec{F} = -\frac{1}{2}\,\rho(r) v^2 C_D A\,\hat{\tau} \tag{29}$$

$$\rho(r) = \rho_0 \exp\left(-\frac{r - R_E - 175km}{H}\right) \tag{30}$$

$$H = \frac{900 + 2.5\,(F10-70) + 1.5A_p}{27 - 0.012(r - R_E - 200km)} \tag{31}$$

Where ρ is the atmospheric density, v is the orbital velocity, C_D is the drag coefficient (taken to be 2.2/mass), A is the front-facing area of the spacecraft (taken to be 0.06 m^3), ρ_0 is the atmospheric density at 175km (taken to be $6*10^{-10}$ kg/m^3), F10 is the solar radio ten centimeter flux (taken to be 70), and A_p is the geomagnetic index (taken to be 0). The force has no out-of-plane direction so $\dot{\Omega} = \dot{I} = 0$. Transforming the force vector in Gauss's variational equations with components aligned to the velocity vector and setting all other force components to zero we get:[7]

$$\dot{a} = \frac{2}{n}\sqrt{\frac{1+e\cos E}{1-e\cos E}} F_\tau \tag{32}$$

$$\dot{e} = \frac{2(1-e^2)\cos E}{an\sqrt{1-e^2\cos^2 E}} F_\tau \tag{33}$$

$$\dot{I} = 0 \tag{34}$$

$$\dot{\omega} = \frac{2}{na}\,\frac{\sqrt{1-e^2}}{e}\,\frac{\sin E}{\sqrt{1-e^2\cos^2 E}} F_\tau \tag{35}$$

$$\dot{\Omega} = 0 \tag{36}$$

$$\dot{M} = -\frac{2}{ane}\,\frac{(1-e^3\cos E)\sin E}{\sqrt{1-e^2\cos^2 E}}\, F_\tau \tag{37}$$

This is very difficult to integrate without making assumptions such as a small eccentricity. There are several works that provide some solution to the contraction of an eccentric orbit due to drag, however these are done through a change in coordinate system, such as the KS orbital elements. As of writing this paper, the author knows of no simple solution or semi-analytic approximation for a highly eccentric orbit. For the supercluster mission case, it is possible

to use the already found Gauss's variational equations for a velocity-tangent force and numerically integrate over a year of orbits to see if there is any change. Upon doing so it is apparent that the air drag has such a small effect it is not worth considering in the rest of the analysis, as seen in Table 5.

Table 5. Orbital Element Variations from Air Drag for a single satellite and the relative change in orbital elements between two satellites in a 50km formation orbit.

Element	Center Satellite Relative to Unperturbed	Corner Satellite Relative to Center
$\dot{a}$ (km/year)	-0.427	-1.118
$\dot{e}$ (year^{-1})	-1.965*10^{-6}	-5.099*10^{-6}
$\dot{I}$ (rad/year)	0	0
$\dot{\omega}$ (rad/year)	0	0
$\dot{\Omega}$ (rad/year)	0	0
$\dot{M}$ (rad/year)	0	0

C. $\dot{M}$ matching

Particularly due to the J2 perturbation, there is a significant drift in the mean anomaly between each satellite. In the 50km formation case this comes out to 0.00297 radians per year, which results in a physical drift of 207km per year of the corner satellite at apogee from the target position. It is relatively simple to account for this drift without the use of thrusters – one can choose the initial semimajor axis of each satellite in the formation such that the relative $\dot{M}$ drifts are equal. As a first pass, the expressions for $\dot{M}$ can be combined to solve for the required semimajor axis for each satellite.

$$\dot{M}_{center\ drift} + n_{center} = \dot{M}_{corner\ drift} + n_{corner} \tag{38}$$

$$n = \sqrt{\frac{\mu}{a^3}} \tag{39}$$

$$a_{corner} = \left(\frac{\mu}{\left(n_{center} + \dot{M}_{center\ drift} - \dot{M}_{corner\ drift}\right)^2} \right)^{\frac{1}{3}} \tag{40}$$

As the $\dot{M}_{corner\ drift}$ is dependent on the semimajor axis of the corner satellite this expression must be numerically calculated for the exact solution, however from a first order pass this changes the semimajor axis of the corner satellite by only 28 m.

D. Delta V Calculations

Previous work by Edalbaum[8] presented the basis for optimal steering algorithms for continuous thrusting quasi-circular orbits, which laid much of the groundwork for many analyses since. More recently J. Pollard wrote on low-thrust maneuver algorithms[3], which provides a great framework to base delta V calculations upon. Following Gauss's

version of Lagrange's Planetary Equations, one can solve the expected change in orbital elements by a thrusting force. Table 6 shows the expressions for Delta V which have been either found in this reference, or the reference used as a basis to determine the Delta V for large eccentricity orbits. For these large eccentricity orbits, a closed form analytic solution was only possible by assuming the thrust was performed as a series of small impulsive maneuvers about the apogee.

Table 6. Delta V Calculations for Low-thrust correction of orbital elements

Element	Delta V Calculation	
a	$\left\lvert \sqrt{\frac{\mu}{a_0}} - \sqrt{\frac{\mu}{a_1}} \right\rvert \left(\frac{1+e}{\sqrt{1-e^2}} \right)$	Ref [8]
e	$\frac{2}{3}\sqrt{\frac{\mu}{a}} \lvert arcsin\, e - arcsin(e + \Delta e) \rvert$	Ref [3]
I	$\sqrt{\frac{\mu}{a}} \left\lvert \frac{\sqrt{1-e^2}}{1+e} \frac{\Delta I}{\cos \omega} \right\rvert$	Ref [8]
ω	$\frac{2}{3}\sqrt{\frac{\mu}{a}} \frac{e}{\sqrt{1-e^2}} \lvert \Delta\omega \rvert$	Ref [8]
Ω	$\frac{\pi}{2}\sqrt{\frac{\mu}{a}} \lvert \sin I \ \Delta\Omega \rvert$	Ref[8]
M	N/A due to $\dot{M}$ matching	

Here we have assumed the semimajor axis, eccentricity, and inclination changes are performed by a series of small impulsive thrusts about the apogee, while ω and Ω are continuous thrusts.

Table 7. Delta V's required to counteract orbital element changes

Element	J2 Perturbation Delta V (m/s/year)	Moon Perturbation Delta V (m/s/year)	Sun Perturbation Delta V (m/s/year)
$\dot{e}$	0	0	0
$\dot{I}$	0	0	0
$\dot{\omega}$	1689	86	0.02
$\dot{\Omega}$	2869	34	0.01

As can be seen there are several expressions that would be infeasible to completely counteract with thrusters. For example, trying to maintain the argument of perigee ω and longitude of right ascension would require impractical amounts of fuel. However by allowing the orbit to slowly precess and instead ensuring the orbital elements relative to each satellite remains constant – that is, allowing the entire formation to precess while retaining the shape – the fuel requirements become much more reasonable. The total relative change in orbital elements for the 50km satellite formation case is shown in Table 8, as well as the Delta V/year required to counteract these changes.

Table 8. Total Relative Change in Orbital Elements for different satellite formation sizes and Delta V required to counteract relative change

Element	50km Formation	
	Relative Change	Delta V (m/s/year)
$\dot{a}$		0.15
$\dot{e}$	$5.01*10^{-6}$ /year	0.00
$\dot{I}$	$6.674*10^{-6}$ rad/year	0.01
$\dot{\omega}$	$3.063*10^{-3}$ rad/year	23.19
$\dot{\Omega}$	$1.546*10^{-3}$ rad/year	39.37

In total, for a 3-year mission at least 200 m/s Delta V is required to maintain the formation. Fuel requirements for a 8kg satellite is dependent on the specific impulse of the thruster. As the station-keeping is expected to be the smaller part of the total Delta V required, the analysis of the orbit transfer must be completed first and used to determine the appropriate thruster class.

IV.Low-Thrust Orbit Transfer

Unlike high-thrust propulsion, there are no analytic expressions for low-thrust orbital transfers. While this makes determining the Delta V's and mission time quite difficult and requiring extensive numerical simulations, a relatively fast method for an approximation of the mission can be found using the method initially developed by E. Burk[4], and later by J. Pollard[3]. Their method involved solving the time-dependent changes in orbital elements given a low-thrust orbital perturbation due to a thruster. This provides an analytic expression for the time dependent orbital elements given a thruster firing in any direction for some amount of time centered around the perigee or apogee. This can then be numerically extrapolated to simulate how the orbit changes given the thruster firing pattern and once the desired orbit is reached, the Delta V and time taken can be determined. The only inputs into such a simulation are then: angle of orbit which the thruster is firing, the magnitude of the thrust, and the direction the thruster is facing. What is key in this simulation, however, is the angle from the perigee/apogee α. The change in orbit element per orbit is very dependent on this quantity, as seen in Figure 5.

Table 9. Secular orbital element changes over each steering case.

	Steering 1) Perpendicular to the orbit radius vector	Steering 2) Tangent to the orbit path	Steering 3) Perpendicular to the major axis of the ellipse
$\frac{da}{dt}$	$\frac{2f}{\pi}\sqrt{\frac{a^3}{\mu}(1-e^2)}\alpha$	$\frac{2f}{\pi}\sqrt{\frac{a^3}{\mu}}\int_0^{\alpha}\sqrt{1-e^2\cos^2 E}\,dE$	$-\frac{2\sigma f}{\pi}\sqrt{\frac{a^3}{\mu}(1-e^2)}\sin\alpha$
$\frac{de}{dt}$	$\frac{2f}{\pi}\sqrt{\frac{a}{\mu}(1-e^2)}(4\sigma\sin\alpha + 3e\alpha + e\cos\alpha\sin\alpha)$	$\frac{2f}{\pi}\sqrt{\frac{a}{\mu}}(1-e^2)H(\sigma,\alpha)$	$\frac{f}{2\pi}\sqrt{\frac{a}{\mu}(1-e^2)}(4\sigma e\sin\alpha + 3\alpha + \cos\alpha\sin\alpha)$

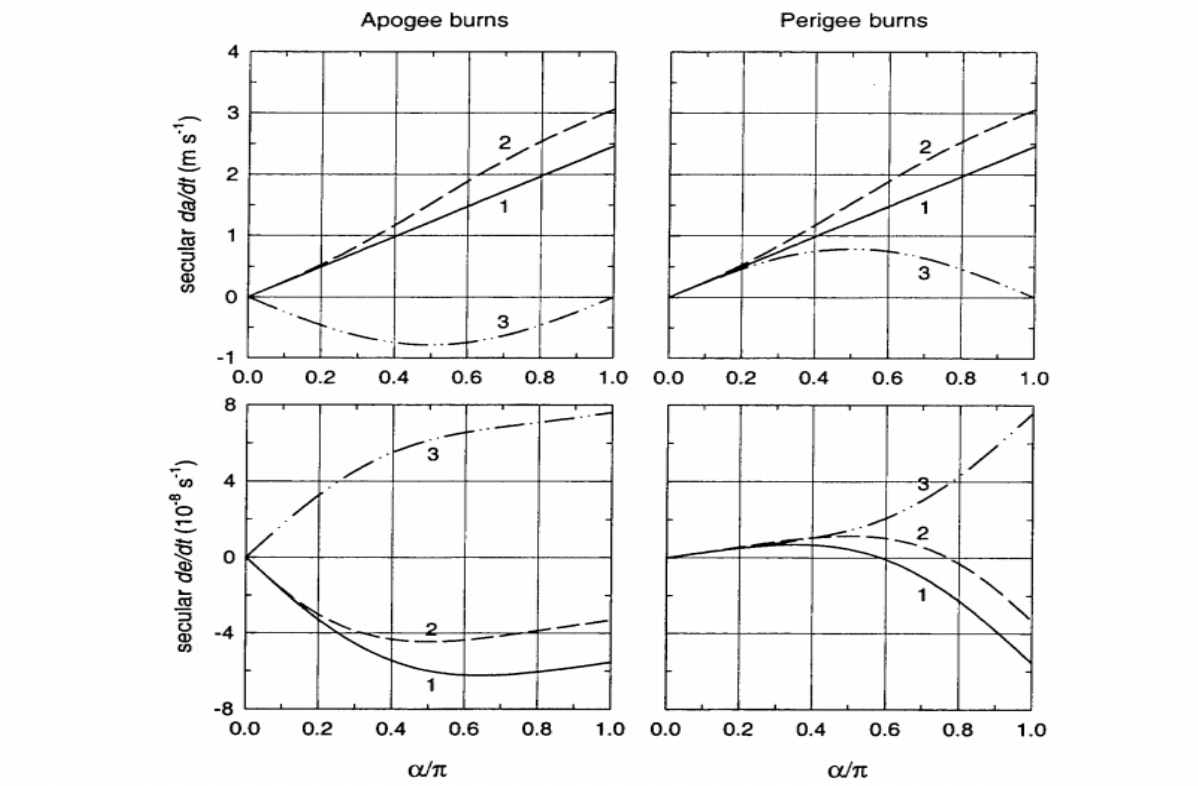

Figure 5. Comparison of in-plane steering cases (1), (2), and (3) in a geosynchronous transfer orbit with an apogee altitude of 35,768 km and perigee altitude of 185km.[4]

Another important input is the direction of the thruster. In the model provided by Pollard and Burk, simple expressions can be obtained for the secular change in orbital elements based on 3 different thrusting schemes: 1) Thrust perpendicular to the orbit radius vector, 2) thrust tangent to the orbit path, and 3) thrust perpendicular to the major axis of the ellipse. Figure 5 shows the effect these in-plane steering cases.
Knowing how these orbital elements change with each steering scheme and burn arc α provides a quick method to determine a rough timeline and DeltaV needed to get to any target orbit by first thrusting at one angle to get to an intermediate orbit where some orbital elements reach their target, and then another angle to hold those elements constant to reach the final target orbital elements.

Following a steering case 2 – steering case 3 method, the time and Delta V required for the orbital transfer was determined by a forward-Euler numerical simulation. This was performed for two cases: one where the satellites start in an ISS orbit (400km altitude) and thrust to the final orbit, and another where they are placed in a geo-transfer orbit and thrust to the final orbit. A graphical representation of the steering scheme can be seen in Figure 6.

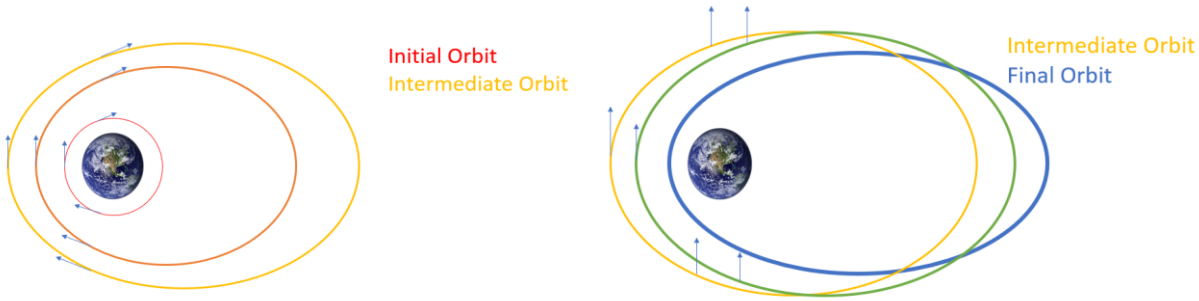

Figure 6. Graphical Representation of the thrusting scheme and orbit maneuvers of the simple algorithm

The time taken to complete the maneuvers from both an initial ISS orbit and Geo-Transfer Orbit, the fuel mass needed for both it and station-keeping, as well as a basic cost analysis are shown in Table 10. These numbers include a buffer of 600m/s of Delta V of fuel. The three scenarios are shown in Figure 7.

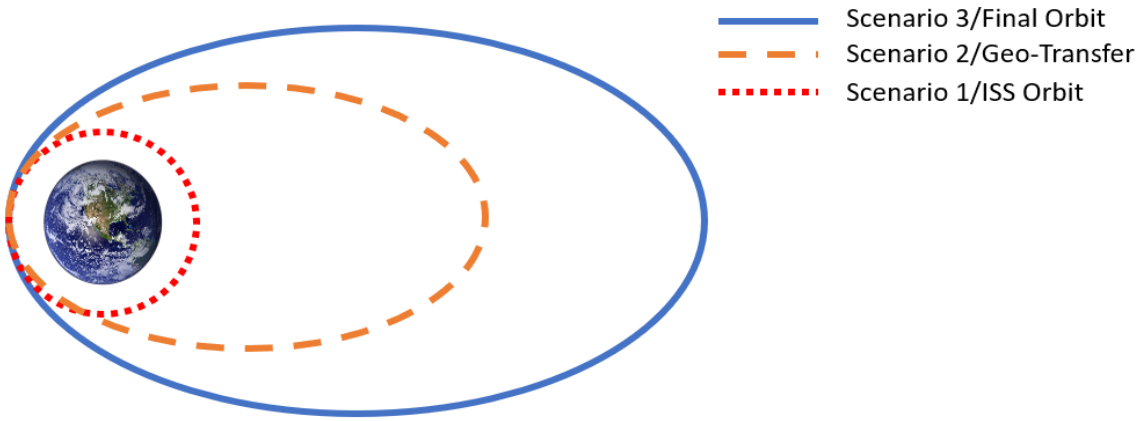

Figure 7. The three scenarios performed for the Delta V calculation and cost analysis. Scenario 1: Deploy from ISS Orbit and maneuver to final orbit. Scenario 2: Deploy from GTO and maneuver to final orbit. Scenario 3: Deploy from final orbit

The Delta V for scenario 1 was found to be 4035 m/s while the Delta V for scenario 2 was 608 m/s. Scenario 1 appears prohibitively high unless a high specific impulse thruster, such as a Hall Thruster, is used. However, a 6U CubeSat is only capable of generating so much power through deployed solar panels before heating becomes an issue. Commercially available solar panels offer a maximum of ~100 W for such satellite classes. If these were continually charging a battery over the orbit, and discharged while the thruster fires over the orbit angle α – which is roughly half the orbit while transferring – a rough estimate of 200W thruster power can be assumed. With an efficiency of 40%, then by selecting the specific impulse the thrust of the thruster can be calculated along with the expected time such a transfer would take. This becomes a tradeoff between transfer time and fuel mass – a value of 1500 s specific impulse was chosen here for all scenarios.

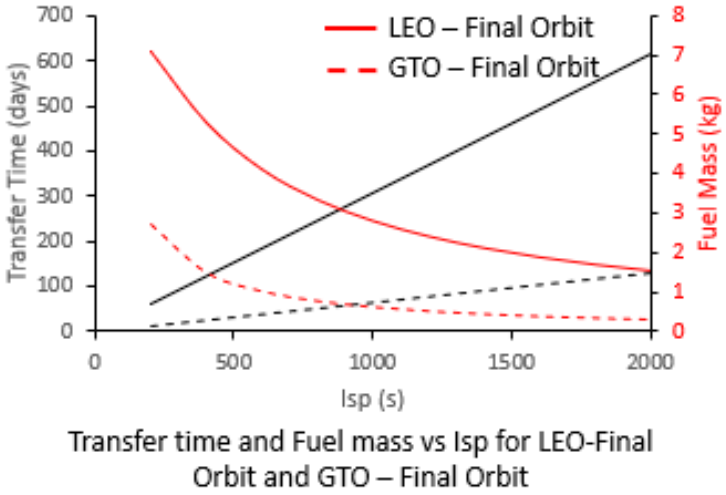

Transfer time and Fuel mass vs Isp for LEO-Final Orbit and GTO – Final Orbit

Figure 8. Transfer time and Fuel mass vs Isp for LEO-Final Orbit and GTO-Final Orbit

$$Thrust = \frac{\eta P_{in}}{2\, Isp * g} = 10.9\, mN \qquad (41)$$

Table 10. Launch Cost, Time Requirements, Fuel Mass, and Total Cost for three scenarios

	Launch Cost (million)	Third Stage Time (days)	Mass needed for fuel (kg)	Satellite Cost (million)	Total Cost (million)
Scenario 1	$ 4.4	462	2.00	$ 24	$ 28.4
Scenario 2	$ 11.2	97	0.43	$ 24	$ 35.2
Scenario 3	$ 17.9	0	0.11	$ 24	$ 41.9

Combining the orbit transfer and formation maintenance provides an initial estimate of the total Delta V and corresponding fuel mass required for each 8 kg satellite in the formation, shown in table 10. Using cost estimates of launching CubeSats as a secondary payload from SpaceFlight Industries[9], expected cost of satellite development from previous proposals,[10] a simple cost analysis for 3 cases is found and shown in table 10. Case 1 is for a rocket launch from Earth to a LEO orbit of 400km and an onboard thruster transfer from 400km circular orbit to the final orbit. Case 2 is for a rocket launch from Earth to a common super-synchronous orbit used to place geostationary satellites (GTO), with the onboard thrusters taking the rest of the journey to the final orbit. Case 3 is for a dedicated rocket launch to the final orbit with no low-thrust transfer. All cases include the delta V and corresponding fuel for formation-keeping.

CubeSats are limited by a certain mass/volume by the launch provider, which tends to stand at ~1.33kg/U, where 1U is 10cm x 10cm x 10cm. Thus with a set satellite size there is an upper limit on the total mass for the satellite, which in our analysis results in a tradeoff between payload mass and fuel mass. Table 10 reveals it is much more cost effective to use the onboard thrusters to transfer from a cheaper low Earth orbit, however this comes at the expense of payload mass and time.

V.Conclusion

With a reliable electric propulsion system that can achieve thrusts of 10.9 mN with 40% efficiency and with onboard electronics that can sustain 15 months of radiation during transit it is possible to save $13.5 million by sending the cubesats as secondary payloads on existing Earth-LEO small satellite launch systems. Given that thruster lifetime can be limiting and electronics lifetime is a significant concern due to radiation, two alternate cases of using a larger orbit or a dedicated launcher is also analyzed and can ameliorate these risks for the price of $35.2 million and $41.9 million respectively. Several candidates for the electric propulsion system exist, both on the market and in development, and have varying advantages. Using the low power Cylindrical Hall Thruster, for instance, presents great savings in mass and the ability for higher thrusts, however it is relatively untested. Using the commercially available Indium FEEP thruster provides some reliability, but the mission times will be extended due to the lower thrust capability. Further analysis is needed to understand the effect of radiation damage during the orbit transfer which may filter out several of the existing options.

Acknowledgments

This work is partially supported by the United States DOE. The authors would like to thank Dr. Jeremy Kasdin for several fruitful discussions.

References

[1] M. Yamada et al “Proc. COSPAR 2017”, Korea (2017)

[2] C. Tooley, University of North Dakota Space Studies Colloquium 2015

[3] J. E. Pollard, "Simplified Analysis of Low-Thrust Orbital Maneuvers," *Aerospace Report NO.,* Vols. TR-2000, no. 8565-10, 2000.

[4] E. Burt, "On space manoeuvres with continuous thrust," *Planetary and Space Science,* vol. 15, no. 1, pp. 103-122, 1967.

[5] R. D. C. Domingos, R. Vilhena de Moraes and A. F. B. A. Prado, "Third-Body Perturbation in the Case of Elliptic Orbits for the Disturbing Body," *Mathematical Problems in Engineering,* vol. 129, no. 3, 2008.

[6] "Earth Atmosphere Density Approximations," Australian Space Academy, [Online]. Available: https://www.spaceacademy.net.au/watch/debris/atmosmod.htm.
[7] S. Klioner, Lecture Notes on Basic Celestial Mechanics, 2011.
[8] T. Edelbaum, "Propulsion Requirements for Controllable Satellites," *ARS Journal,* vol. 31, no. 8, 1961.
[9] "Spaceflight - Scheduling and Pricing," Spaceflight Industries, 2 July 2019. [Online]. Available: http://spaceflight.com/schedule-pricing/#pricing.
[10] L. Kepko & G. Le, "Magnetospheric Constellation: Tracing the flow of mass and energy from the solar wind through the magnetosphere," NASA Goddard Space Flight Center